

Experimental Investigation of Static Friction Coefficient between Vehicle Tyre and Various Road Conditions

M.F. Ezzat^a, M.A. Mourad^{a,b} and M.M. Yousef^a

^aMechanical Engineering Dept.,

Faculty of Engineering, Minia University, Egypt.

^bCorresponding Author, Email: m.mourad@mu.edu.eg

ABSTRACT:

The static friction force increases for an increase in the tangential displacement up to the value that is necessary to initiate gross-sliding of the bodies in contact. The static friction coefficients of tyre tread of different strength properties under varying contact conditions are investigated. Smooth surfaces were considered to evaluate the effects of roughness on adhesion of tyre treads. In this investigation different types of road surfaces were tested. The results show that larger tread contact resulted in higher coefficients of static friction. The static friction coefficient decreased for an increase in the tyre tread stiffness. The static friction coefficient decreased for an increase in the surface roughness, then passes through a minimum and finally increased for higher roughness of the counter face. The effect of contaminants such as water, fuel and lubricant between head and counter face were also investigated.

KEYWORDS:

Static friction coefficient; Tyre tread; Contact pressure; Road surface roughness; Contamination

CITATION:

M.F. Ezzat, M.A. Mourad and M.M. Yousef. 2014. Experimental Investigation of Static Friction Coefficient between Vehicle Tyre and Various Road Conditions, 6(1-2), 1-7. doi:10.4273/ijvss.6.1-2.01.

1. Introduction

During macroscopic rest state of bodies, a micro-slip occurs at the interface between bodies and then processed to macro-sliding situation. This micro-slip can reach relatively large values when one of the surfaces in contact has a low tangential stiffness compared to the other surface. The main parameters of the static friction regime are the maximum static friction force at which macro-sliding initiates and the corresponding micro-displacement. Once the bodies are set in motion, certain force is required to sustain it in the dynamic friction regime [1]. Few mechanisms have been found responsible for static friction. These mechanisms might involve elastic or plastic deformation of the softer material in contact and asperity creep [1, 2]. They will be presented for the contact between metals as well as for the contact between rubber and metal.

In the experimental investigation carried out by Deladi [1], the influence of normal load, geometry and rubber-like material stiffness on the Static Friction Coefficient (SFC) have been undertaken. The results showed that larger radii of the ball resulted in higher coefficients of static friction and related this behaviour was related to an increase in the contact area. The results also showed that the SFC decreased for stiffer materials and this behaviour was related to the decrease in contact area of the stiffer materials. The third observation was that the SFC decreased with normal load and at lower loads this decrease was more significant than at higher loads. This was alone confirmed by Maziar et al. [3].

Abdel-Halim [4] showed that under the condition of constant contact load the friction coefficient displayed by rubber decreased for an increase in the contact area. For hard rubber, the friction coefficient increased for an increase in the contact area. The first was related to the deformation component of friction. The second was related to the adhesion component of friction. Besides the two previously mentioned factors Gabriel et al. [5] confirmed an additional third geometric factor through the experimental work validated by finite element analysis. This contribution is dependent on the penetration depth of the rigid surface into the elastomeric. This geometric contribution considerably increases the actual coefficient of friction. This was previously observed by Laing et al. [6], but was not fully investigated.

Experiments were carried out by Barquins for rubber/glass contact [7, 8]. The preliminary stage of friction was studied experimentally. The evaluation of the contact area was carried out using a central adhesive zone that is surrounded by an annulus of slip. Adachi [9] carried out experiments on rubber balls in contact with glass plates and revealed that the process of partial slip and its propagation with increasing tangential load. The static friction force was investigated by Roberts and Thomas [10] for smooth rubber hemispheres in contact with glass plates. Their experiments suggested that the magnitude of the static friction force is related to the elastic deformation of rubber. Persson [11] found that the molecular group of rubber chemically attached to the top solid was responsible for the static friction in rubber.

According to the theoretical models [12-14], the contact area between two spheres under combined normal and tangential loading consists of a central stick region surrounded by an annular slip zone. As the tangential load increases, the central stick region gradually diminishes and finally disappears. At this moment gross sliding begins which satisfies the Coulomb friction law. Barquins and Roberts [15] showed that the SFC decreases if the normal load increases. The dependence of the micro-displacement on the SFC was studied by Bogdanovich and Baidak [16]. They showed that the limiting displacement increases linearly with the SFC and this relationship becomes non-linear at higher pressures. Bogdanovich and Baidak [16] investigated the effect of surface roughness on the SFC between a polymer plate and a steel cylinder. They found that the limiting displacement decreases with increasing average roughness (R_a) of the steel counter body, then passes through a minimum and finally increases for higher R_a . This phenomenon causes different problems such as noise, squeal and wear.

The friction between tyre and road is based on adhesion and deformation [17-20, 31]. The adhesion component of elastomeric friction has been found to be inversely proportional to the hardness and contact pressure and might be considered as a viscoelastic dependent. The mechanism of deformation can be described as a bulk phenomenon which has its ultimate effect at the sliding interface and depends chiefly on the nature of the macro-roughness or the micro-roughness of the counter face and in addition proportional to contact pressure [19]. The maximum value of the coefficient of sliding friction depends on the type and state of the road, rubber hardness, and viscoelastic properties, tread design, degree of tread wear, tyre inflation pressure, the normal load taken by the wheel and its camber [21, 22]. Furthermore, the vertical load and air pressure were found to influence the grip coefficient significantly in longitudinal and lateral directions at different constructions of tyre tread. The wheel camber was found to have significant influences on tyre grip coefficient especially for the wider tyre due to the effective change between tyre and road surface. The influence of air pressure and the vertical load on tyre grip coefficient was investigated in [23-30]. In this paper the SFCs in longitudinal and lateral directions of tyre tread over epoxy, cement and asphalt counter faces are investigated using laboratory tests. The effect of contact pressure, tread stiffness and counter face contaminants are also assessed.

2. Experimental work

Tests were carried out using a test rig designed to measure the tangential static friction force and the applied normal load. Their values were displayed directly on digital screens; one of the screens was connected to a load cell positioned vertically to measure the static friction force, whilst the second was positioned horizontally to measure the normal load as shown in Figs. 1 and 2. One side of the loading pan was prepared to carry the loads and the other side to fix the tyre treads.

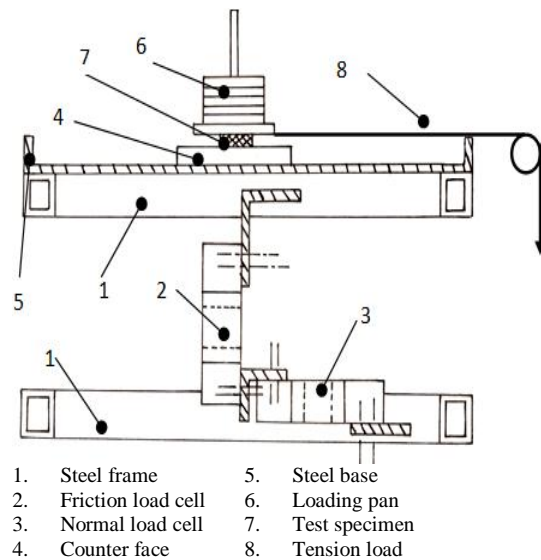


Fig. 1: Schematic layout of the test rig

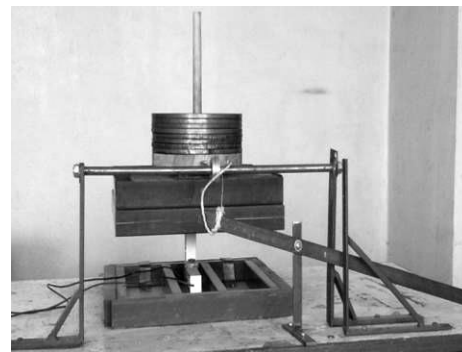


Fig. 2: Layout of the test rig

The vehicle tyre tread is shown in Fig. 3. The tangential friction force was applied directly through a rope, one end of which was connected to the loading pan by means of a hook and the other to a lever arm with a 1:3 ratio. Road surface materials were seated over the base of the test rig. The base was connected firmly to the friction load and normal force load cells. The load cells together with the connected digital screens form two complete strain calibrated bridges. Smooth and rough road surfaces were examined. The smooth surfaces were of ceramic and epoxy flooring to study the effect of roughness on the adhesion of tyre treads. Road test specimens were of asphalt and cement tyre treads of different hardness were used to study the effect of tyre hardness on SFC. Road test specimens contaminated with water, fuel and lubricant oil were examined.



Fig. 3: Vehicle tyre treads

3. Results and discussions

Fig. 4 shows the relationship between the SFC and contact pressure for tyre tread with 77 shore A hardness, at dry condition in the longitudinal direction. The examined surfaces were epoxy surface of $R_a = 0.26 \mu\text{m}$ and $.47 \mu\text{m}$ and ceramic surface of $R_a = 5.47 \mu\text{m}$. The results show that the SFC decreases slightly with increasing contact pressure. As the R_a increases from $0.26 \mu\text{m}$ to $0.47 \mu\text{m}$, the SFC increases. The reason is explained by the increase of the deformation component of friction due to energy dissipation of rubber after deformation by the ruggedness of the counter face. Fig. 5 shows the relation between SFC and contact pressure for tyre tread with 66 shore A hardness, at dry condition and in the longitudinal direction. The examined surfaces were epoxy surface of $R_a = 0.36 \mu\text{m}$ and $0.92 \mu\text{m}$ and ceramic surface of $R_a = 7.93 \mu\text{m}$. The results show that friction coefficient decreases with increasing contact pressure. Furthermore, the SFC has been observed to increase with increasing R_a due to the effect of the deformation component of friction. This has been observed up to the contact pressure of 2.46 bar. However, as the contact pressure increases no further substantial difference in the results is recorded.

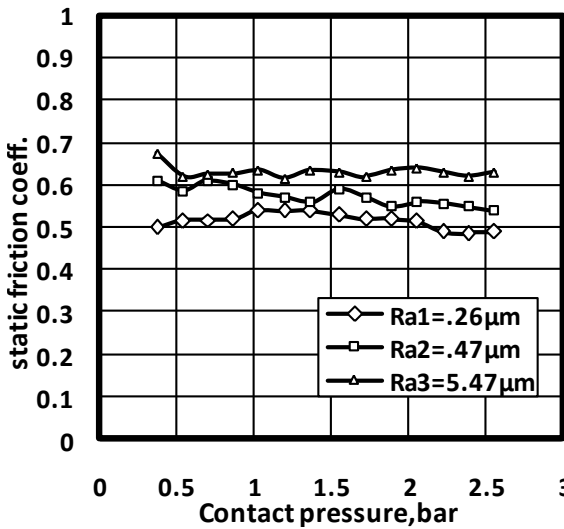


Fig. 4: Effect of surface roughness, R_a , on SFC, hard tread over epoxy surface

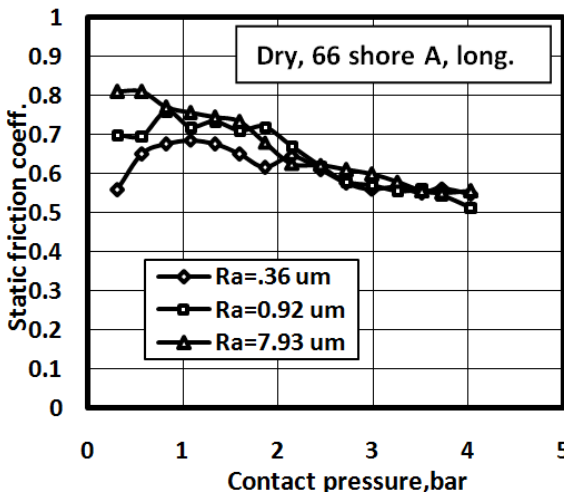


Fig. 5: Effect of surface roughness, R_a , on SFC, soft tread over epoxy surface

Fig. 6 illustrates the effect of the contact pressure on the SFC for different tread hardness in the longitudinal direction. The counter face was hard epoxy surface with $R_a = 0.31 \mu\text{m}$. Tests were carried out under dry operating conditions. For 77 shore A hardness, the tread became stiffer and decreased the contact area. This has reduced the supported tangential load and hence the static friction force and friction coefficient. The test results supported this rationale and showed that the SFC for softer tread is larger. Fig. 7 shows the effect of R_a on SFC at different contact pressure in the longitudinal direction and under dry condition. Initially, the SFC increases for an increase in R_a up to $0.92 \mu\text{m}$. After this, the SFC decreases with increasing R_a of the counter face then passes through a minimum and finally increases for higher R_a . Adhesion effects decreases when R_a increases due to reduction of the number and size of the treads in contact, leading to a drop in friction level. At higher R_a , the ploughing component of friction increases with R_a , as a result, the SFC also increased.

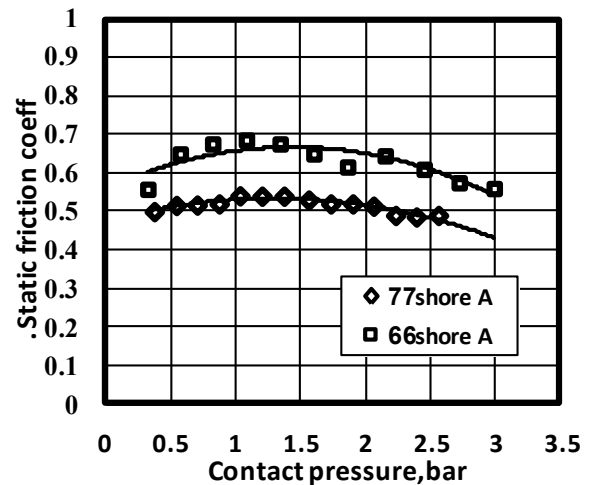


Fig. 6: Effect of tyre tread stiffness on SFC, hard epoxy surface

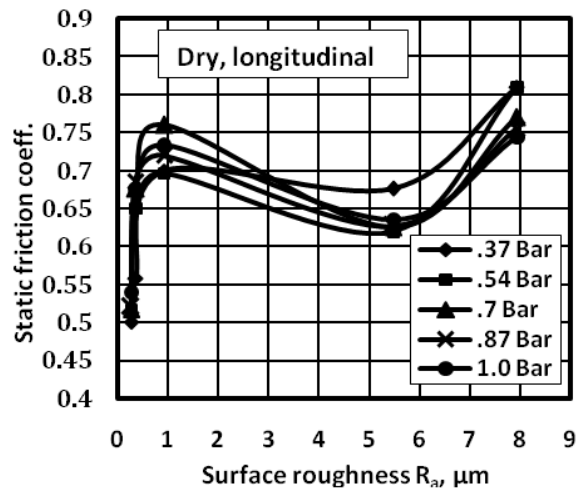


Fig. 7: Effect of surface roughness, R_a , on SFC under dry conditions

Fig. 8 shows the relationship between the SFC and contact pressure for tyre treads specimens of 66 shore A and 77 shore A hardness. For cement counter face tests were carried out in the longitudinal direction and under dry condition. The soft tyre tread of 66 shore A hardness displayed higher SFC than hard tread. However, for

contact pressures higher than 2.6 bar the soft and hard treads displayed no variation in friction coefficients. This is due to a gradual increase in the stiffness of the soft tread with increasing contact pressure. This behaviour is accompanied by decrease in the tangential force supported by the contact area. Fig. 9 shows the effect of the interface contact area of the 77 shore A tyre tread on the SFC in the longitudinal direction for the counter face dry cement surface. Larger contact area displayed higher SFC than the smaller area. The SFC decreased with increase in the contact pressure which attributed to the decrease of the adhesion component of friction.

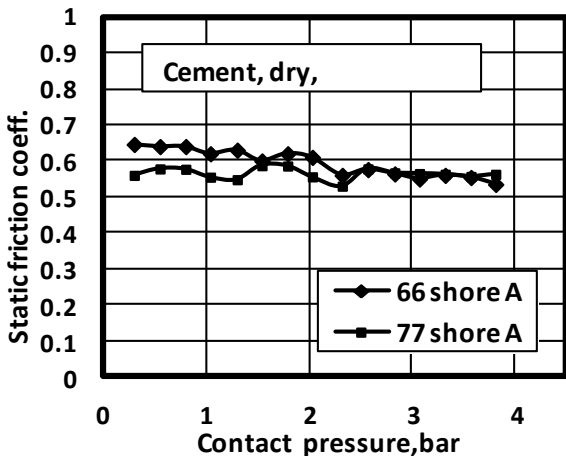


Fig. 8: Effect of tread stiffness on SFC over cement surface

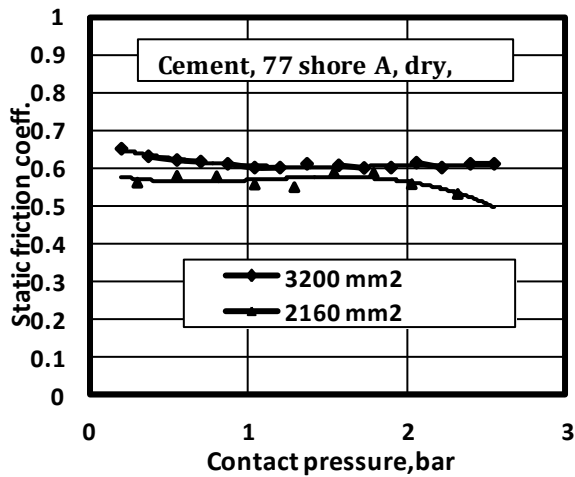


Fig. 9: Effect of tread interface area on SFC, cement surface

Figs. 10 and 11 show a comparison of SFC in lateral and longitudinal directions over cement surface for 66 and 77 shore A treads under dry conditions. The SFCs displayed higher values in lateral direction than in longitudinal direction. The friction coefficient decreased with increasing the contact pressure. The soft tread of 66 shore A showed higher SFC compared with hard tread of 77 shore A hardness.

Fig. 12 shows the effect of tyre tread stiffness on SFC of asphalt counter face under dry condition in longitudinal direction for 66 and 77 shore A treads. Soft tread displayed a modest increase in friction coefficient than hard tread. The soft and hard treads displayed a decrease in friction coefficient with increasing contact pressure. Furthermore, asphalt counter face showed higher friction coefficients than cement counter face.

Fig. 13 shows the relation between the SFC in longitudinal and lateral directions for 66 shore A tread. The contact surface was asphalt and the tests were carried out under dry conditions. The SFCs displayed higher values in lateral direction than in longitudinal direction. The friction coefficient decreased with increasing the contact pressure. The difference between the SFCs in lateral and longitudinal directions for soft and hard treads is nearly the same.

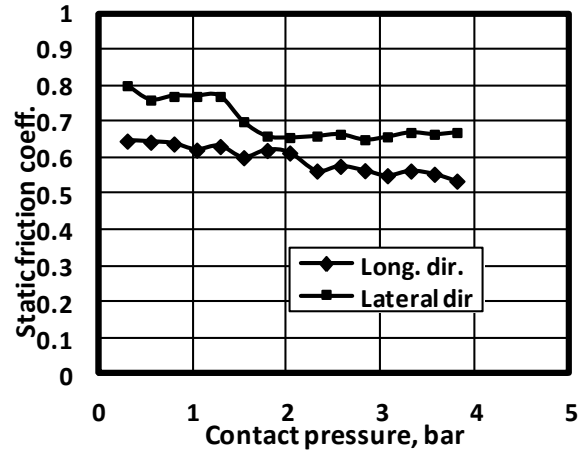


Fig. 10: Comparison between SFC in longitudinal and lateral directions over cement surface for 66 Shore A tread

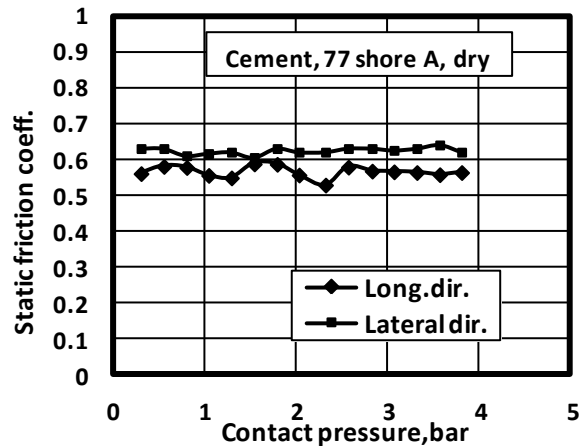


Fig. 11: Comparison between SFC in longitudinal and lateral directions over cement surface 77 shore A tread

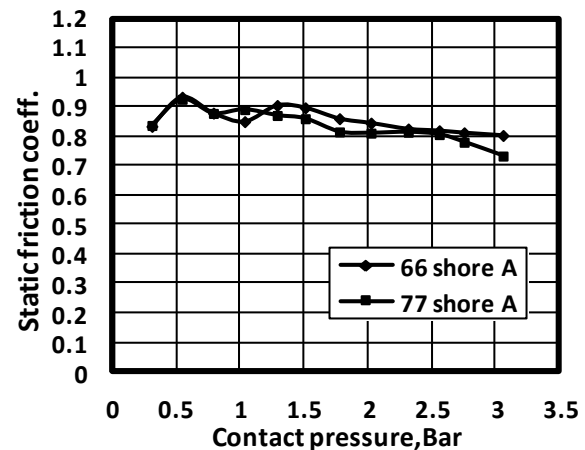


Fig. 12: Effect of tread stiffness on SFC, asphalt surface

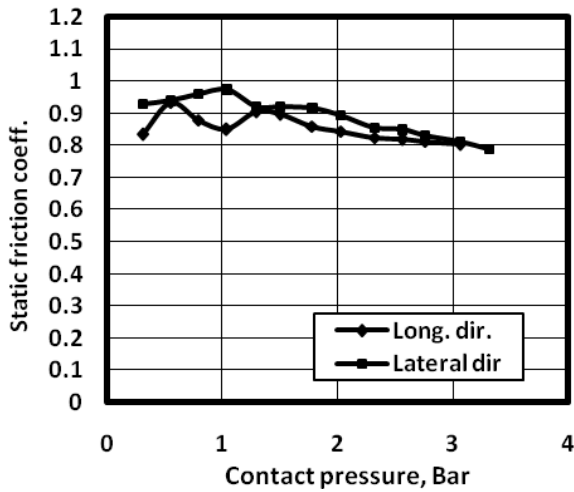


Fig. 13: Comparison between SFC in long. and lateral direction over asphalt surface for 66 shore A tread

Fig. 14 shows the relation between the SFC and the contact pressure up to 4 bars for tread with 66 shore A hardness in the longitudinal direction. The counter face was ceramic with $R_a = 7.5 \mu\text{m}$. The results showed that the SFC decreased with increasing the lubrication of the contaminant. The contaminants form layers of low shear strength properties and the tangential force required to rupture these layers would be small. The SFC was observed to decrease with increasing contact pressure.

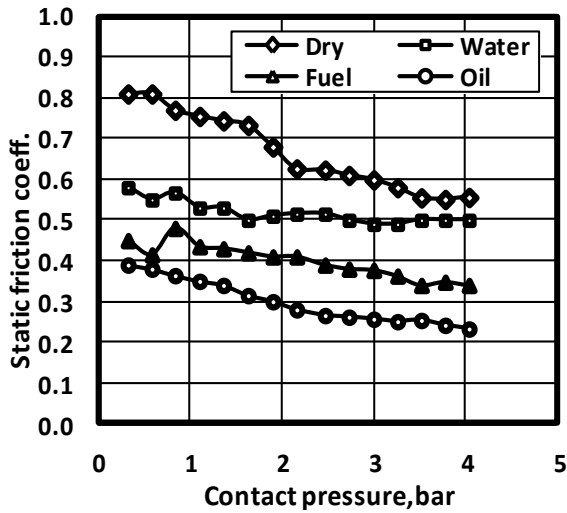


Fig. 14: Effect of contaminants on SFC, soft tread over hard ceramic surface

Figs. 15 and 16 show the relation between the SFC at different contaminated conditions for 66 and 77 shore A tyre treads. The counter face was cement and the friction coefficient was measured in the longitudinal direction. Wet, fuel and oil contaminants were investigated. For soft tyre tread, the maximum SFCs were displayed under dry contact conditions, whilst the oil lubricated interface showed the lowest values of SFCs. At contact pressures higher than 2.5 bar, the soft tread displayed an equal value of friction coefficients. This behaviour is accompanied by decreasing the tangential force supported by the contact area. The SFCs decreased with increasing contact pressure. The lower SFCs displayed with oil lubricating condition are due to low shear strength of the oil layer. The hard tyre tread

test results displayed low SFCs compared with soft tyre tread due to decrease in contact area of the hard tread. The interface contaminated with water displayed a slight decrease in SFCs than the dry contact for hard tread. The interface contaminated with oil film displayed a considerable decrease in SFC due to the appreciable lubrication of oil.

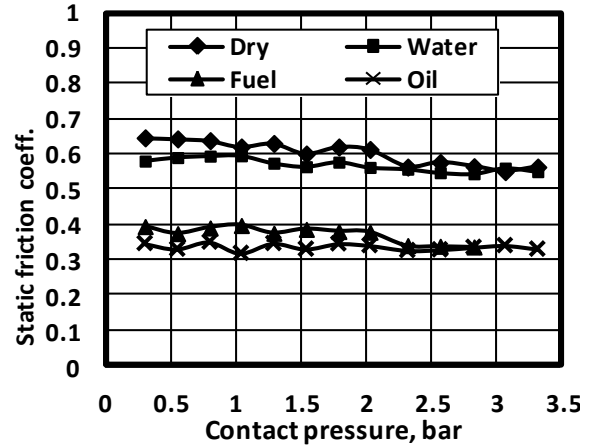


Fig. 15: Effect of different contaminants on SFC, soft tread over cement surface

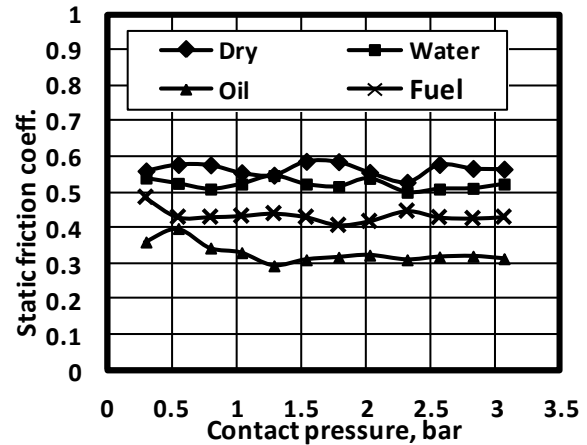


Fig. 16: Effect of different contaminants on SFC, hard tread over cement surface

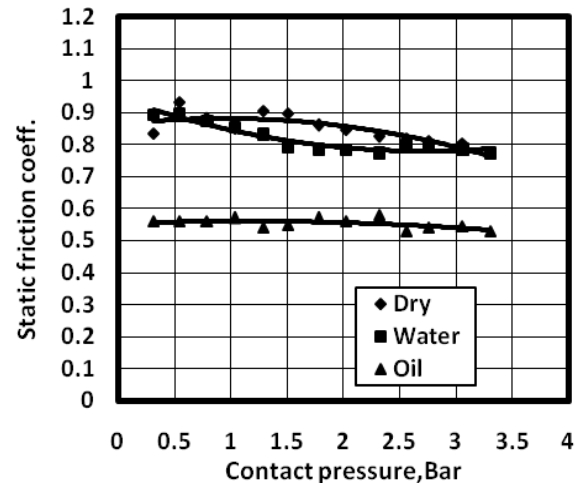


Fig. 17: Effect of different contaminants on SFC, soft tread over asphalt surface

Figs. 17 and 18 show the relation between the SFC at different contaminated conditions for 66 and 77 shore

A tyre treads. The counter face was asphalt and the friction coefficient was measured in the longitudinal direction. For 66 shore A soft tread, the maximum SFCs were displayed under dry contact conditions, whilst the oil lubricated interface showed the lowest values of SFCs. The interface contaminated with oil displayed a substantial decrease in SFC due to the low shear strength of the oil layer. For hard tyre tread specimen of 77 shore A, the test results displayed low SFCs compared with soft tyre tread. The interface contaminated with water displayed a slight decrease in SFCs. The interface contaminated with oil film displayed a substantial decrease in SFC due to the appreciable lubrication of oil.

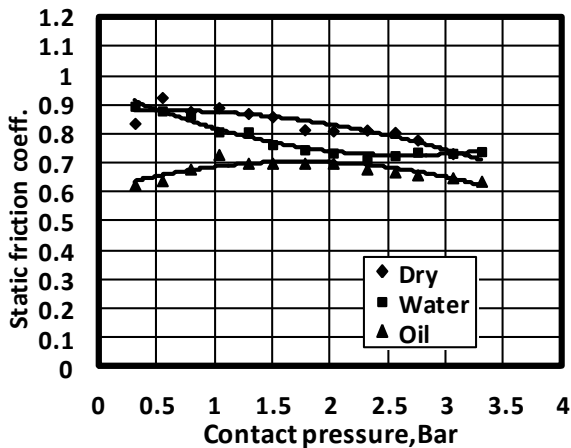


Fig. 18: Effect of different contaminants on SFC, hard tread over asphalt surface

4. Conclusions

The SFC was found to decrease with increasing Ra, then passes through a minimum and finally increased for higher Ra of the counter face friction. The SFCs displayed higher values in lateral direction than in longitudinal direction. This may depend on the form of the contact patch and grooves of the tread. The SFC decreased with increasing the lubrication of the contaminants. With higher shore A hardness, the contact area decreased determining a reduction of the supported tangential load, hence the static friction force and friction coefficient also decreases.

REFERENCES:

- [1] E. Deladi. 2006. *Static Friction in Rubber-Metal Contacts with Application to Rubber Pad Forming Process*, PhD Thesis, University of Twente, Netherlands.
- [2] J. Galligan and P. Cullough. 1985. On the nature of static friction, *Wear*, 105, 337-340. [http://dx.doi.org/10.1016/0043-1648\(85\)90232-7](http://dx.doi.org/10.1016/0043-1648(85)90232-7).
- [3] M. Ramezani, M. Ripin and R. Ahmad. 2009. Computer aided modeling of friction in rubber pad forming process, *J. Materials Processing Technology*, 209, 4925-4934. <http://dx.doi.org/10.1016/j.jmatprotec.2009.01.015>
- [4] A. Abdel-Halim. 2009. *Tribological Behavior of Rubber Sliding Against Engineering Surfaces*, PhD Thesis, Minia University, Egypt.
- [5] P. Gabriel, A. Thomas and J. Busfield. 2010. Influence of interface geometry on rubber friction, *Wear*, 268, 747-750. <http://dx.doi.org/10.1016/j.wear.2009.11.019>.
- [6] H. Liang, Y. Fukahori, A.G. Thomas and J. Busfield. 2009. Rubber abrasion at steady state, *Wear*, 266, 288-296. <http://dx.doi.org/10.1016/j.wear.2008.07.006>.
- [7] M. Barquins. 1992. Adherence, friction and wear of rubber-like materials, *Wear*, 158, 87-117. [http://dx.doi.org/10.1016/0043-1648\(92\)90033-5](http://dx.doi.org/10.1016/0043-1648(92)90033-5).
- [8] M. Barquins. 1993. Friction and wear of rubber-like materials, *Wear*, 160(1), 1-11. [http://dx.doi.org/10.1016/0043-1648\(93\)90400-G](http://dx.doi.org/10.1016/0043-1648(93)90400-G).
- [9] K. Adachi, K. Kato, J. Liu and H. Kawamura. 2004. The effect of contact morphology on initiation and propagation of micro-slip at contact interface, *Proc. ASME/STLE Int. Joint Tribology Conf.*, California, USA.
- [10] A. Roberts and A. Thomas. 1979. Static Friction of smooth clean vulcanized rubber, *NR Technology*, 7(2), 38-42.
- [11] B. Persson, O. Albohr, F. Mancosu, V. Peveri, V. Samoilov and I. Sivebaek. 2003. On the nature of the static friction, kinetic friction and creep, *Wear*, 254, 835-851. [http://dx.doi.org/10.1016/S0043-1648\(03\)00234-5](http://dx.doi.org/10.1016/S0043-1648(03)00234-5).
- [12] E.L. Deladi, M.B. de Rooij and D.J. Schipper. 2007. Modeling of static friction in rubber-metal contact, *Tribology Int.*, 40, 588-594. <http://dx.doi.org/10.1016/j.triboint.2005.11.007>.
- [13] R.D. Mindlin. 1994. Compliance of elastic bodies in contact, *ASME J. Appl. Mech.*, 16, 259-268.
- [14] W.R. Chang, I. Etsion and D.B. Bogy. 1988. Static friction coefficient model on metallic rough surfaces, *ASME J. Tribol.*, 110(1), 57-63. <http://dx.doi.org/10.1115/1.3261575>.
- [15] M. Barquins and A. Roberts. 1986. Rubber friction variation with rate and temperature: some new observations, *J. Phys. D: Appl. Phys.*, 19, 547-563. <http://dx.doi.org/10.1088/0022-3727/19/4/010>.
- [16] P. Bogdanovich and A. Baidak. 2002. Micro-slip in metal-polymer friction pairs, *J. Friction and Wear*, 23(3), 41-45.
- [17] M. Kroger, K. Popp and N. Kemdzirra. 2004. Experimental and analytical investigation of rubber adhesion, *Machine Dynamics Problems*, 28(1), 79-89.
- [18] W. Sextro. 2002. *Dynamical Contact Problems with Friction*, Lecture Notes in Applied Mechanics, Springer Bevlm, Heidelberg, New York. <http://dx.doi.org/10.1007/978-3-540-46871-4>.
- [19] F. Desmond. 1972. *The Friction and Lubrication of Elastomers*, Pergamon Press.
- [20] H. Kummer. 1966. *Unified Theory of Rubber and Tire Friction*, Engg. Research Bulletin, B-94, Penn. State University.
- [21] M. Artamonov, V. Ilarionov and M. Morin. 1976. *Motor Vehicles Fundamental and Design*, Mir Publishers.
- [22] I. Rosen, R. Rusev and P. Ichev. 2006. Laboratory investigation of tire sliding grip coefficient, *Transport*, XXI(3), 172-181.
- [23] J. Wong. 1984. *Theory of Ground Vehicles*, John Wiley & Sons, London.
- [24] S. Choi, J. Bang, M. Cho and Y. Lee. 2002. Sliding mode control for anti-lock system of passenger vehicles featuring electro-rheological valves, *IMechE Part D: J. Automobile Engineering*, 216(11), 897-900. <http://dx.doi.org/10.1243/095440702321031441>.
- [25] S. Clark. 1970. *Mechanics of Pneumatic Tires*, National Highway Traffic Safety Administration, USA.

- [26] K. Guo. 1994. The effect of longitudinal force and vertical load distribution on tire slip properties, *SAE Paper 945087*.
- [27] R. Kamnik, F. Boettiger and K. Hunt. 2003. Roll Dynamics and lateral load transfer estimation in articulated heavy freight vehicle, *IMechE Part D: J. Automobile Engineering*, 217(11), 985-997. <http://dx.doi.org/10.1243/095440703770383884>.
- [28] C. Mousseau and S. Clark. 1994. An analytical and experimental study of a tire rolling over a stepped obstacle at low velocity, *Tire Science and Technology*, 22(3), 162-181. <http://dx.doi.org/10.2346/1.2139540>.
- [29] C. Oertel. 1996. On modeling contact and friction calculation of tire response on uneven roads, *Vehicle System Dynamics*, 27(1), 289-302. <http://dx.doi.org/10.1080/00423119708969661>.
- [30] M. Varat, J. Kerkhoff, S. Husher, C. Armstrong and K. Shuman. 2003. The analysis and determination of tire roadway frictional drag, *SAE Paper 2003-01-0887*.
- [31] S.D. Sarker. 1980. *Friction and Wear*, Academic Press.